Journal of the Mechanics and Physics of Solids 58 (2010) 636–655

Contents lists available at ScienceDirect

Journal of the Mechanics and Physics of Solids

journal homepage: www.elsevier.com/locate/jmps

Dynamic crack growth under Rayleigh wave

Leonid I. Slepyan *

School of Mechanical Engineering, Tel Aviv University, Israel

ARTICLE INFO

Article history:
Received 2 September 2009
Received in revised form
3 December 2009
Accepted 9 March 2010

Keywords:
Dynamic fracture
Intermittent crack growth
Elastic material
Integral transforms
Asymptotic analysis

ABSTRACT

A nonuniform crack growth problem is considered for a homogeneous isotropic elastic medium subjected to the action of remote oscillatory and static loads. In the case of a plane problem, the former results in Rayleigh waves propagating toward the crack tip. For the antiplane problem the shear waves play a similar role. Under the considered conditions the crack cannot move uniformly, and if the static prestress is not sufficiently high, the crack moves interruptedly. For fracture modes I and II the established, crack speed periodic regimes are examined. For mode III a complete transient solution is derived with the periodic regime as an asymptote. Examples of the crack motion are presented. The crack speed time-period and the time-averaged crack speeds are found. The ratio of the fracture energy to the energy carried by the Rayleigh wave is derived. An issue concerning two equivalent forms of the general solution is discussed.

1. Introduction

Dynamic crack growth under the action of a harmonic wave was first examined in the problem of a uniform lattice with a uniformly propagating crack (Slepyan, 1981). In such a steady-state regime, the crack speed coincides with the phase speed, $v=\omega/k$ (ω is the frequency and k is the wavenumber), and the latter speed must be below the group velocity, $v<v_g=\mathrm{d}\omega/\mathrm{d}k$; otherwise, the wave cannot deliver the energy to the crack to grow. Note that for any periodic lattice there exists a range of frequencies where the inequality, $v<v_g$, is satisfied. Recently a lattice with a low density interface layer embedded into the uniform structure was examined in Mishuris et al. (2009). In such a waveguide, there exists a localized harmonic wave, which can be excited by a remote local load. The existence of the steady-state regime studied analytically was confirmed by numerical simulations. The latter also allowed an established crack-speed oscillation regime to be revealed. In Slepyan et al. (2009), in addition to these regimes for the lattice, a dynamic crack in a flexural plate was considered. This continuous model is also characterized by an anomalous dispersion of waves localized at the crack faces (in this model, $v_g=2v$), and the crack under the action of a sinusoidal wave can grow uniformly.

In the present paper, the harmonic—wave-propagating crack problem is considered for a homogeneous elastic medium. In the latter, there is no wave dispersion, that is, the equality, $v=v_g$, is valid for Rayleigh waves localized at a half-plane boundary as well as for longitudinal and shear waves, and hence the uniform crack propagation is impossible. Nonuniformity makes the task much more difficult, and though some aspects of the interaction of Rayleigh waves with a crack were discussed long ago (Freund, 1981; Rossmanith and Fourney, 1981), it seems that this problem has not yet been sufficiently investigated.

The first general solution to the transient, nonuniform crack speed problem, where the crack face traction was not specified, was found by Kostrov (1966) for mode III. The plane problem solution for the subcritical crack speed,

* Tel.: +972 3 640 6224; fax: +972 3 640 7617.
E-mail address: leonid@eng.tau.ac.il

0022-5096/$ - see front matter © 2010 Elsevier Ltd. All rights reserved.
doi:10.1016/j.jmps.2010.03.003

$v(t)=\mathrm{d}l(t)/\mathrm{d}t<c_R$, was obtained by Freund (1972, 1973) (here and below $l(t)$ is the crack tip coordinate, c_R is the Rayleigh wave speed). Then the general plane problem solution was obtained by Kostrov (1974, 1975) for the sub-Rayleigh crack speeds, $v(t)<c_R$ and for the range $c_R<v(t)<c_2$ (Kostrov, 1976) (c_2 is the shear wave speed). Slepyan (1974) using a different technique had obtained a more general solution to such a mixed problem (also see Saraikin and Slepyan, 1979; Slepyan, 2002). In the context of the present paper, it is important that in the latter solution both the traction at $x<l(t)$ and the displacement at $x>l(t)$ could be arbitrarily assigned. The same technique has then been used by Slepyan and Fishkov (1980) for a more complicated regime in which the speed of the nonuniformly moving separation point may cross the critical values, c_R, c_2 and c_1. This topic was also considered in the papers by Willis (1990) and Walton and Herrmann (1992). The nonuniformly moving mode III interface crack was examined by Leise (2005). Various aspects of crack dynamics are considered, in particular, in the books by Freund (1990), Broberg (1999), Slepyan (2002) and Ravi-Chandar (2004).

In the plane problem, the general expressions for the stresses ahead of the crack and for the crack face displacements are complicated; these quantities are expressed in terms of a fourfold integral, not counting an integral representation of a crack-speed-independent function. Although the energy release rate relations generally contain only a twofold integral, as the *loading function*, which reflects the crack growth history, the expression is still not easy in use.

Due to the symmetry the fracture-mode-related displacement on the crack continuation is equal to zero, and the usual crack-dynamics formulations, obtained in the above-mentioned works in more or less extent of generality and completeness, are mainly based on the crack-face traction as the input action. There is, however, another form of the general solution based on the displacement caused by this load. It is shown below in Section 4.2 that these two forms are equivalent; however, the latter is more suitable in the case of a remote load. It turns out that for the action of a sinusoidal wave the displacement-based loading function can be asymptotically calculated. Briefly stated, the twofold integral is shown to be asymptotically equal to the double, Laplace and Fourier, integral transform of a crack-speed-independent function. Fortunately this *LF*-transform has a simple expression. As a result, an implicit first-order nonlinear differential equation is found, which is expressed in terms of the current crack tip position and speed. This equation governs an established, periodic, dynamic crack growth. The energy fracture criterion is used and analytical and numerical results following from this equation are presented.

In the problem formulation, it is assumed that the crack faces are traction free. This cannot be immediately applied to mode I, where the pure wave action leads to crack closure. To avoid this phenomenon, the combined action of the harmonic wave and a sufficiently high static prestress which would rule out crack-closure is assumed.

Along with the plane problem, mode III fracture is also considered. In the latter case, the transient problem has an explicit solution, and it can be seen how fast the latter and its periodic-crack-speed asymptote approach each other.

At first, some background material concerning plane and Rayleigh waves is presented. Then the problem is formulated and a superposition scheme to be used in the analysis is discussed. General relations for the nonuniform dynamic crack growth are further shown. Recall that in general, the crack growth is governed by a first-order differential equation which contains a function of the crack tip coordinate expressed by a twofold convolution integral reflecting the crack growth history. For the considered sinusoidal loading a crucial simplification is obtained as an explicitly expressed function instead of the integral. Analytical dependencies and calculation results are presented. In particular, examples of the crack motion, time-averaged crack speed relations, and the ratio of the fracture energy to the energy carried by the Rayleigh wave are shown.

According to the solution, as the load intensity increases, the current and the averaged crack speeds tend to the incident wave speed, as it should. It is well known, however, that the crack motion becomes unstable approximately at a half of the Rayleigh wave speed, and this imposes a real restriction on the averaged crack speed (see Ravi-Chandar and Knauss, 1984; Fineberg et al., 1991, 1992; Marder and Liu, 1993; Marder and Gross, 1995; Willis and Movchan, 1997; Fineberg and Marder, 1999; Ravi-Chandar, 2004). At the same time, in the case of the crack propagating along a weak interface, the crack speed can approach the Rayleigh wave speed (Ravi-Chandar and Knauss, 1984; Lee and Knauss, 1989). In the present paper, the crack propagation instability is not considered; however, the known instability bound can be introduced into the crack speed governing relations in the same way as the non-negative crack speed condition.

2. Plane and Rayleigh waves in outline

The homogeneous isotropic elastic medium is characterized by a couple of elastic parameters λ and μ or μ and ν, where μ and ν are the shear modulus and Poisson's ratio, respectively. In terms of the latter couple, $\lambda=2\mu\nu/(1-2\nu)$. The material density is denoted by ϱ.

Dynamics of the medium is governed by two wave equations with respect to the scalar and vector potentials, ϕ and $\boldsymbol{\psi}$

$$\Delta\phi-\frac{1}{c_1^2}\ddot{\phi}=0,\quad \Delta\boldsymbol{\psi}-\frac{1}{c_2^2}\ddot{\boldsymbol{\psi}}=0, \tag{1}$$

where c_1 and c_2 are longitudinal and shear wave speeds, respectively

$$c_1=\sqrt{\frac{\lambda+2\mu}{\varrho}}=\sqrt{\frac{2(1-\nu)\mu}{(1-2\nu)\varrho}},\quad c_2=\sqrt{\frac{\mu}{\varrho}}. \tag{2}$$

The displacement vector and stress tensor can be expressed in terms of the above potentials as follows:

$$\boldsymbol{u}=\boldsymbol{\nabla}\phi+\boldsymbol{\nabla}\wedge\boldsymbol{\psi},$$

$$u_x=\frac{\partial\phi}{\partial x}+\frac{\partial\psi_z}{\partial y}-\frac{\partial\psi_y}{\partial z},$$

$$\sigma_{xx}=\lambda\Delta\phi+2\mu\left(\frac{\partial^2\phi}{\partial x^2}+\frac{\partial^2\psi_z}{\partial x\partial y}-\frac{\partial^2\psi_y}{\partial z\partial x}\right),$$

$$\sigma_{xy}=\sigma_{yx}=\mu\left(2\frac{\partial^2\phi}{\partial x\partial y}+\frac{\partial^2\psi_z}{\partial y^2}-\frac{\partial^2\psi_z}{\partial x^2}+\frac{\partial^2\psi_x}{\partial z\partial x}-\frac{\partial^2\psi_y}{\partial y\partial z}\right). \tag{3}$$

Expressions for the remaining components of the displacements and stresses follow from this by cyclic permutation: $x\to y\to z\to x$.

The longitudinal and shear plane sinusoidal waves propagating in x-direction have the following complex representation:

$$u_x=\frac{\partial\phi}{\partial x}=AE,\quad E=\exp[\mathrm{i}(\omega t-kx)],\quad \omega=c_1k \tag{4}$$

and

$$\left\{u_y=\frac{\partial\psi_x}{\partial z}-\frac{\partial\psi_z}{\partial x},\quad u_z=\frac{\partial\psi_y}{\partial x}-\frac{\partial\psi_x}{\partial y}\right\}=A_{(y,z)}E,\quad \omega=c_2k, \tag{5}$$

respectively. This medium is with no wave dispersion, and hence it admits not only the sinusoidal wave, but also waves in which displacements are defined by an arbitrary function of the variable $x-c_{1(2)}t$.

In an elastic half-plane ($y>0$ or $y<0$) with a traction free boundary, there exist *Rayleigh wave* exponentially localized at the vicinity of the half-plane boundary. For the upper half-plane the two elastic potentials are given in this case by

$$\phi=\frac{\mathcal{A}}{k\sqrt{\alpha_1^2-\alpha_2^2}}\exp[-k\alpha_1y+\mathrm{i}(\omega t-kx)],$$

$$\psi_z=-\frac{\mathrm{i}(1+\alpha_2^2)\mathcal{A}}{2k\alpha_2\sqrt{\alpha_1^2-\alpha_2^2}}\exp[-k\alpha_2y+\mathrm{i}(\omega t-kx)],\quad \psi_x=\psi_y=0, \tag{6}$$

where $\mathcal{A}$ is the wave amplitude at y=0, and the parameters α and β are

$$\alpha_1=\sqrt{1-(c_R/c_1)^2},\quad \alpha_2=\sqrt{1-(c_R/c_2)^2},\quad \omega=c_Rk. \tag{7}$$

The Rayleigh wave speed, c_R, satisfies the equation

$$(1+\alpha_2^2)^2-4\alpha_1\alpha_2=0,\quad 0<c_R<c_2. \tag{8}$$

The below expression for c_R/c_2 as a function of Poisson's ratio

$$\frac{c_R}{c_2}\approx 0.8740+0.2004\nu-0.07567\nu^2 \tag{9}$$

is a very accurate approximation. The dependence is shown in Fig. 1 (the difference between exact and approximate dependencies is indistinguishable).

The displacement vector, $\boldsymbol{u}(u_x,u_y)$, is defined by its components as

$$u_x=\frac{\mathrm{i}\mathcal{A}}{2\sqrt{\alpha_1^2-\alpha_2^2}}[-2\exp(-k\alpha_1y)+(1+\alpha_2^2)\exp(-k\alpha_2y)]E,$$

$$u_y=\frac{\mathcal{A}}{2\alpha_2\sqrt{\alpha_1^2-\alpha_2^2}}[-2\alpha_1\alpha_2\exp(-k\alpha_1y)+(1+\alpha_2^2)\exp(-k\alpha_2y)]E. \tag{10}$$

Using identity (8) the amplitudes of these components at y=0 can be found as

$$A=A_x=|u_x|=\sqrt{\frac{\alpha_2}{\alpha_1+\alpha_2}}\mathcal{A},\quad A=A_y=|u_y|=\sqrt{\frac{\alpha_1}{\alpha_1+\alpha_2}}\mathcal{A}. \tag{11}$$

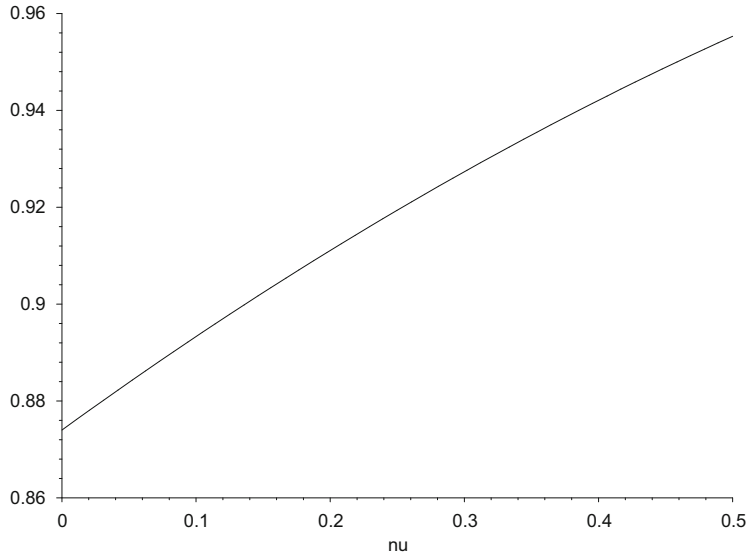

Fig. 1. The normalized Rayleigh wave speed, c_R/c_2, as a function of Poisson's ratio.

The stresses are

$$\sigma_{xx}=\frac{\mu k\mathcal{A}}{\sqrt{\alpha_1^2-\alpha_2^2}}[-(1-\alpha_2^2+2\alpha_1^2)\exp(-k\alpha_1 y)+(1+\alpha_2^2)\exp(-k\alpha_2 y)]E,$$

$$\sigma_{yy}=\frac{\mu k\mathcal{A}(1+\alpha_2^2)}{\sqrt{\alpha_1^2-\alpha_2^2}}[\exp(-k\alpha_1 y)-\exp(-k\alpha_2 y)]E,$$

$$\sigma_{xy}=\frac{2\mathrm{i}\mu k\mathcal{A}\alpha_1}{\sqrt{\alpha_1^2-\alpha_2^2}}[\exp(-k\alpha_1 y)-\exp(-k\alpha_2 y)]E. \tag{12}$$

There is no wave dispersion in this case too, and the energy flux velocity in the wave, which is equal to the group velocity, coincides with the Rayleigh wave speed, c_R. An expression for the energy flux in the Rayleigh wave is presented in Section 7.

The surface wave of an arbitrary shape can be expressed as

$$u_{x,y}(x,y,t)=f_{x,y}(x-c_R t)g_{x,y}(y),\quad g_x(0)=g_y(0)=1. \tag{13}$$

It follows from (6) that if one of the displacement component at $y=0$, f_x or f_y, is given, then the other functions in (10) and (12) are uniquely defined.

3. Formulation

In an infinite, uniform, isotropic elastic medium, there exists a semi-infinite crack, $x<0$, $y=0$. At $t=0$ a wave propagating from the left reaches the crack tip, and beginning from this moment it forces the crack to grow along the x-axis. The task is to find how the current and averaged crack speeds depend on wave amplitude and what part of the energy flux in the wave is spent on fracture.

3.1. A remote load and the wave

We consider the case where the harmonic wave is excited by a crack-face load applied far enough from the crack tip. It is reasonable, in this case, to take the wave displacements on the crack faces as the input action and to omit the remote load description. This provides a greater generality and, at the same time, simplifying the problem. With this in mind we based on the general solution given by Slepyan (1974) (also see Saraikin and Slepyan, 1979; Slepyan, 2002), where a possible nonzero displacement on the crack continuation is taken into account. In the considered problem, the displacement is assumed to be of the same value but opposite to the wave displacement. Thus the original zero-displacement condition is satisfied. Clearly, the solution obtained in this way must coincide with that obtained in the 'usual' way where the load is considered as the input action, and this is true regardless of the type of load. This issue is

discussed in more detail in Section 4.2, where it is shown that the load-based and the displacement-based formulations are equivalent, and the latter is only suitable for the remote load expression of the former. (The general solution accepted here becomes more important in a more general mixed problem, where the nonuniformly moving point really separates the boundary conditions expressed in terms of the load and nonzero displacements.)

3.2. The wave configuration

In the considered fracture problem, it is assumed that the Rayleigh wave propagating to the right on the upper half-plane, i.e. the wave localized at the upper crack face, is defined as the imaginary part of the complex wave (10)

$$\boldsymbol{u}^{\uparrow} = \Im \boldsymbol{u}(x,y,\alpha_1,\alpha_2) \quad (y>0). \tag{14}$$

The same wave is valid for the lower half-plane if signs of α_1 and α_2 are changed

$$\boldsymbol{u}_{\downarrow} = \Im \boldsymbol{u}(x,y,-\alpha_1,-\alpha_2) \quad (y<0). \tag{15}$$

This wave configuration corresponds to mode I, since the normal component, u_y, is antisymmetric with respect to y, whereas $u_x(-y)=u_x(y)$, and this latter component does not influence the crack growth. In the opposite case

$$\boldsymbol{u}_{\downarrow} = -\Im \boldsymbol{u}(x,y,-\alpha_1,-\alpha_2) \quad (y<0), \tag{16}$$

$u_x(-y)=-u_x(y)$, $u_y(-y)=u_y(y)$, and hence the latter wave configuration (14), (16) corresponds to mode II. In the following, the arrows are omitted.

In application to mode III, it is assumed that the non-localized incident shear waves are

$$u_{\mathrm{III}} = A\sin(\omega t-kx) \ \ (y>0), \quad u_{\mathrm{III}} = -A\sin(\omega t-kx) \ \ (y<0). \tag{17}$$

3.3. Superposition

Due to the symmetry only the upper half-plane, $y>0$, can be considered. It is convenient to represent the fracture mode-related displacement by the superposition of three fields. At $y=0$ the first one corresponds to the incident wave freely propagating in the half-plane

$$u^{(1)}(x,0,t) = A\sin[\omega(t-x/c)]H(t-x/c), \quad \boldsymbol{\sigma}^{(1)}(x,0,t) = 0, \tag{18}$$

where for modes I and II c is the Rayleigh wave speed, $c=c_R$, and for mode III c is the shear wave speed, $c=c_2$; $u^{(1)}$ is the y, x or z component of the displacement vector for modes I, II and III, respectively, $\boldsymbol{\sigma}$ is the traction and H is the Heaviside unit step function.

For Rayleigh wave such sharp front is, of course, an idealization; it can be valid for the plane wave in mode III only. However, the H-multiplier in (18) is preserved for all fracture modes. For mode III this corresponds to an exact formulation of the transient problem, and this allows to see the transition to the established regime in every detail. For the plane problem the only latter regime is studied and hence the real shape of the Rayleigh wave at arrival does not matter. Note that the first part of the total displacement is regular, and it gives no contribution to the energy release.

The second part corresponds to zero initial conditions and to the following conditions at $y=0$:

$$u^{(2)} = -A\sin[\omega(t-x/c)]H(t-x/c) \quad [x \ge l(t)],$$

$$\boldsymbol{\sigma}^{(2)} = 0 \quad [x<l(t), l(0)=0]. \tag{19}$$

The third part corresponds to a remote static load whose action results in a nontrivial solution of the homogeneous problem with the conditions

$$u^{(3)} = 0 \ \ [x \ge l(t)], \quad \sigma^{(3)} = 0 \ \ [x<l(t)] \tag{20}$$

and with a static stress intensity factor K_0. The superposition gives us the required conditions

$$\sum_{i=1}^{3} \boldsymbol{\sigma}^{(i)} = 0 \ \ [x<l(t)], \quad \sum_{i=1}^{3} u^{(i)} = 0 \ \ [x \ge l(t)], \tag{21}$$

which, together with the incident wave and the static prestress, define the problem formulation for the elastic half-plane.

The incident wave displacement and the static prestress are assumed to be given; hence the determination of the second part constitutes the main problem. Recall, however, that for mode I the static prestress is assumed to be sufficiently large to allow the crack closure to be ignored. The total displacement, $u^{(1)}+u^{(2)}+u^{(3)}$, must be considered in this regard.

4. The main relations

The solution to the considered problem is derived based on a general solution to the related mixed problem presented in the papers mentioned in the Introduction and in Chapter 9 of the book (Slepyan, 2002). In order to facilitate a detailed examination of the subject, the key relations from this book used below will be indicated by using double brackets $[(\cdots)]$.

4.1. General solution

A general mixed problem is considered, where the displacement at $x > l(t)$, $u^+(x,t)$, and the traction at $x < l(t)$, $\sigma^-(x,t)$ are assumed to be given. These components in the opposite supports, $u^-(x,t)$ and $\sigma^+(x,t)$, are the unknown functions. In terms of the Laplace and Fourier transforms

$$u^{LF}(k,s) = \int_{-\infty}^{\infty}\int_{0}^{\infty} u(x,t)\exp(-st+\mathrm{i}kx)\,\mathrm{d}t\,\mathrm{d}x, \tag{22}$$

the respective components of the displacement and traction at $y=0$ are connected by the corresponding dynamic Green's function

$$u^{LF}(k,s) = S^{LF}(k,s)\sigma^{LF}(k,s). \tag{23}$$

In turn we have

$$u^{LF}(k,s) = u_+(k,s)+u_-(k,s), \quad \sigma^{LF}(k,s) = \sigma_+(k,s)+\sigma_-(k,s),$$

$$u_{+(-)}(k,s) = [u^{+(-)}(x,t)]^{LF}, \quad \sigma_{+(-)}(k,s) = [\sigma^{+(-)}(x,t)]^{LF}. \tag{24}$$

To resolve the mixed problem the Wiener–Hopf technique is used. Green's function is factorized as

$$S^{LF}(k,s) = S_+(k,s)S_-(k,s) \quad \text{or} \quad S(x,t) = S^+(x,t) * *S^-(x,t), \tag{25}$$

where the asterisks denote the double convolution with respect to x and t. The supports of $S^{+(-)}(x,t)$ must locate outside the considered range of the speeds; in particular, for the subcritical speeds $(-c_R < v(t) < c_R)$ the factorization type is such that the supports are

$$\operatorname{supp} S^+ : c_R t \le x \le c_1 t, \quad \operatorname{supp} S^- : -c_1 t \le x \le -c_R t \ \ (t>0). \tag{26}$$

The inverse functions are introduced as

$$[P^{+(-)}(x,t)]^{LF} = P_{+(-)}(k,s) = 1/S_{+(-)}(k,s). \tag{27}$$

The functions $P^{+(-)}(x,t)$ have the same supports as $S^{+(-)}(x,t)$, respectively, and

$$S^{+(-)}(x,t) * *P^{+(-)}(x,t) = \delta(t)\delta(x), \tag{28}$$

where $\delta(\cdot\cdot)$ is the Dirac delta function. Note that the *LF*-transform of Green's function, $S^{LF}(k,s)$, has explicit expressions for all the fracture modes.

The solution to the above-described transient dynamic problem is presented in the form [(9.107)]

$$u^- = S^- * *[(S^+ * *\sigma^- - P^- * *u^+ r)H(l(t)-x)+C],$$

$$\sigma^+ = -P^+ * *[(S^+ * *\sigma^- - P^- * *u^+)H(x-l(t))-C]. \tag{29}$$

It is valid if the separation point $x=l(t)$ moves with a speed, $v(t)=\mathrm{d}l(t)/\mathrm{d}t$, which does not cross any critical speed, c_R, c_2, c_1, for example, $-c_R < v(t) < c_R$ or $c_R < v(t) < c_2$ (a more complicated general solution valid without this restriction is presented in Slepyan, 2002, Section 9.5.5). For the subcritical regime, $-c_R < v(t) < c_R$, which is considered here, $C \equiv 0$.

4.2. Crack-face load versus crack-continuation displacements

In this section, we show that the approaches based on the crack-face load and on the crack-continuation displacements are equivalent. First consider a wave propagating along the free boundary of the elastic half-plane. Denote the surface fracture-mode-related component of the displacement by $u^0(x,t)$. Let $x=l(t)$ be the point moving as the crack tip in the fracture problem. Then draw the remote load to a finite distance at the left of this point. So we call the load $\sigma^-(x,t)$. With refer to Eqs. (23)–(25) we represent the double, Laplace and Fourier, transform of the displacements as

$$u^0_+(k,s)+u^0_-(k,s) = S_+(k,s)S_-(k,s)\sigma_-(k,s), \tag{30}$$

where $S(x,t)=S^+(x,t)$ ** $S^-(x,t)$ is Green's function for the half-plane. For the opposite displacement, $u=-u^0$, as the input action in the considered problem, it follows that

$$P_-u_+ = -S_+\sigma_- - P_-u_- \quad (P_\pm = 1/S_\pm). \tag{31}$$

We now find that the second term in the expression (29) is equal to the first one:

$$-(P^- **u^+)H(x-l(t)) = (S^+ **\sigma^- + P^- **u^-)H(x-l(t)) = (S^+ **\sigma^-)H(x-l(t)) \quad [(P^- **u^-)H(x-l(t)) \equiv 0], \tag{32}$$

that is, it leads to the same result as the first one as it should be.

Thus, the approaches based on the load and on the displacement produced by this load are equivalent differing only formally. The latter formulation, however, looks preferable for the case of a remote load since it does not require the load to be introduced and specified. Indeed, if the load support moves away to infinity, in the limit the load 'disappears' but its action as the wave remains. The displacement-based version of the general solution is just suitable for this situation.

Finally, for the classical fracture conditions, where a crack-face traction component and a zero corresponding displacement on the crack continuation are given, there exist two equivalent general solutions

$$u^- = S^- **[(S^+ **\sigma^-)H(l(t)-x)+C],$$

$$\sigma^+ = -P^+ **[(S^+ **\sigma^-)H(x-l(t))-C] \tag{33}$$

and

$$u^- = (u^0)^- + S^- **[(P^- **(u^0)^+)H(l(t)-x)+C],$$

$$\sigma^+ = -P^+ **[(P^- **(u^0)^+)H(x-l(t))-C], \tag{34}$$

where $u^0=(u^0)^+ +(u^0)^-$ is the displacement caused by the load σ^- acting on the initially free half-plane boundary. However, for a remote load, which does not show itself explicitly, only the latter solution remains. The complete representation (29) is more general, it is valid in the case of a more general mixed problem, where both the load at $x < l(t)$ and the *nonzero* total displacement at $x > l(t)$ are given. Also it can be used if a combined load is considered, and different representations are convenient to be used for different types of the load.

4.3. The factors and the energy release rate

The factors for modes I and II are [(9.73), (9.70)]

$$S_+(k,s) = \frac{D_+(k,s)\sqrt{s/c_{1,2}-\mathrm{i}k}}{s/c_R-\mathrm{i}k},$$

$$S_-(k,s) = -\frac{(1-\nu)D_-(k,s)\sqrt{s/c_{1,2}+\mathrm{i}k}}{\mu(s/c_R+\mathrm{i}k)} \tag{35}$$

with

$$D_\pm(\lambda) = \exp\left[\frac{1}{\pi}\int_{c_2/c_1}^1 \frac{f(\alpha)\,\mathrm{d}\alpha}{\alpha \mp c_2/\lambda}\right],$$

$$f(\alpha) = \arctan\frac{4\alpha^2\sqrt{1-\alpha^2}\sqrt{\alpha^2-c_2^2/c_1^2}}{(2\alpha^2-1)^2}, \quad \lambda = \frac{s}{\mathrm{i}k}. \tag{36}$$

Here and below $c_{1,2}=c_1$ (mode I), $c_{1,2}=c_2$ (mode II). For mode III [(9.62), (9.65)]

$$S_+ = \frac{\sqrt{c_2}}{\sqrt{s-\mathrm{i}kc_2}}, \quad S_- = -\frac{\sqrt{c_2}}{\mu\sqrt{s+\mathrm{i}kc_2}},$$

$$S^+ = \frac{\sqrt{c_2}}{\sqrt{\pi}}t_+^{-1/2}\delta(c_2t-x), \quad S^- = -\frac{\sqrt{c_2}}{\mu\sqrt{\pi}}t_-^{-1/2}\delta(c_2t+x),$$

$$P^+ = -\frac{1}{2\sqrt{\pi c_2}}t_+^{-3/2}\delta(c_2t-x), \quad P^-(x,t) = \frac{\mu}{2\sqrt{\pi c_2}}t_-^{-3/2}\delta(c_2t+x), \tag{37}$$

where $t_\pm^{-1/2} = \sqrt{\pm H(\pm t)/t}$, $t_\pm^{-3/2} = \mathrm{d}t_\pm^{-1/2}/\mathrm{d}t$.

In these terms, the energy release rate for modes I–III is [(9.163)]

$$G_{\mathrm{I,II}} = \frac{1-\nu}{\mu}G^0_{\mathrm{I(II)}}(\nu)Q^2[l(t),t],$$

$$G^0_{\mathrm{I(II)}}(\nu) = -\sqrt{\frac{1+\nu/c_{1,2}}{1-\nu/c_{1,2}}}\frac{\nu^2(1-\nu/c_R)^2}{(1-\nu)c_2^2R(\nu)D_+^2(\nu)},$$

$$G_{\rm III}=\frac{1}{\mu}G^0_{\rm III}(v)Q^2[l(t),t],\quad G^0_{\rm III}(v)=\sqrt{\frac{1-v/c_2}{1+v/c_2}},\tag{38}$$

where $v=v(t)$ is the crack speed, $R(v)$ is the Rayleigh function

$$R(v)=(2-v^2/c_2^2)^2-4\sqrt{1-v^2/c_1^2}\sqrt{1-v^2/c_2^2}.\tag{39}$$

and the *loading function* Q is defined below. Note that if the crack resistance depends only on l and $v=\mathrm{d}l/\mathrm{d}t$, the first line in (38) presents an implicit first-order ordinary differential equation; the main task is the determination of the loading function, $Q[l\,(t),t]$.

5. The loading function

In fracture mechanics, the loading function is usually defined as $Q=S^+**\sigma_-$, since the formulation prescribes a zero related component of the displacement ahead of the crack tip (see (29)). For the problem considered here, $u^+=u^{(2)}\not\equiv 0$ (19), and both σ^- and u^+ are to be taken into account in (29). Thus, the function Q in (38) is

$$Q(x,t)=S^+**\sigma^--P^-**u^+.\tag{40}$$

We also use the representation

$$Q=Q_{st}+Q_w,\quad Q_{st}(x,t)=S^+**\sigma^-,\quad Q_w(x,t)=-P^-**u^+,\tag{41}$$

where Q_{st} corresponds to the remote static load. If $v=0$ then $D_+(0)=1$, $\Phi=K\sqrt{\pi/2}$ [(9.126)], and in accordance with [(9.162)] this term can be expressed as

$$Q_{st}[l(t),t]=-\frac{1}{\sqrt{2}}K_0.\tag{42}$$

Note that under this remote action the stress intensity factor depends on the crack speed, $K=K(v)$; however, the loading function is defined by the static value, $K_0=K(0)$, independently of the crack speed.

The wave part of the loading function, Q_w, for modes I and II is

$$Q_w[l(t),t]=A\Im\{\exp[\mathrm{i}\omega(t-l(t)/c_R)]\mathcal{Q}\},$$

$$\mathcal{Q}=\int_0^t\int_{-\infty}^{\infty}P^-(\xi,\tau)H(-\xi-c_R\tau)H(\xi+c_1\tau)\exp[-\mathrm{i}\omega(\tau-\xi/c_R)]H[l(t)-\xi-l(t-\tau)]H[c_R(t-\tau)-l(t)+\xi]\mathrm{d}\xi\mathrm{d}\tau,\tag{43}$$

where the step functions are introduced to show the supports explicitly. Note that $S^{\pm}$ and $P^{\pm}$ are real functions.

The most important point in our considerations is that, in the limit, $t-l(t)/c_R\to\infty$, the latter integral becomes the double, Laplace and Fourier, integral transform, namely

$$\mathcal{Q}\sim P_-(k,s)\quad\text{with } k=\omega/c_R,\ s=0+\mathrm{i}\omega,\tag{44}$$

where $P_-(k,s)=1/S_-(k,s)$ (35), (36).

In order to prove this asymptotic relation, we represent $\mathcal{Q}$ (43) as a sum

$$\mathcal{Q}=\int_0^{\tau_0}(\cdots)\,\mathrm{d}\tau+\int_{\tau_0}^{t}(\cdots)\,\mathrm{d}\tau,\quad \tau_0=\frac{c_Rt-l(t)}{c_1+c_R}.\tag{45}$$

With respect to the first integral it follows from (43) that the support of $P^-(\xi,\tau)$, $-c_1\tau\le\xi\le-c_R\tau$, falls within the integration region. For subcritical crack speeds, $v(t)\le\mathrm{const}<c_R$, $\tau_0\to\infty$ as $t\to\infty$, while the other term tends to zero since the convolution integral converges. It therefore follows from (43) that relation (44) is true.

Referring to (35), (36), the loading function asymptote is found as

$$Q_{w0}=-\frac{K_w}{\sqrt{2}}\sin(\phi+\pi/4),\quad K_w=\frac{2\mu\sqrt{2\omega/c_R}A}{(1-\nu)D_-(c_R)\sqrt{1+c_R/c_{1,2}}},\tag{46}$$

and the total asymptotic value of the loading function is

$$Q=-\frac{1}{\sqrt{2}}[K_0+K_w\sin(\phi+\pi/4)].\tag{47}$$

In the example of mode III crack growth it will be seen that the transient solution approaches the asymptote very soon after the wave arrival.

Finally recall that no crack closure is assumed. It follows that the necessary condition for mode I is

$$K_0\ge K_w.\tag{48}$$

5.1. The wave loading function for mode III

Referring to Eqs. (37) and (43), the exact expression of the loading function can be found as

$$Q_w(l(t),t) = -P^- * * u^+ = A\frac{\mu}{2\sqrt{\pi c_2}}\Im\{\exp[\mathrm{i}\omega(t-l(t)/c_2]\mathcal{Q}\},$$

$$\mathcal{Q} = \int_0^t \int_{-\infty}^{\infty} \tau_+^{-3/2}\delta(c_2\tau+\xi)\exp[-\mathrm{i}\omega(\tau-\xi/c_2)]H[c_2(t-\tau)-l(t)+\xi]H[l(t)-\xi-l(t-\tau)]\,\mathrm{d}\xi\,\mathrm{d}\tau$$
$$= -4\mathrm{i}\sqrt{\omega}\int_0^{\phi/2}\tau^{-1/2}\exp(-2\mathrm{i}\tau)\,\mathrm{d}\tau = -4\mathrm{i}\sqrt{\pi\omega}[C(\sqrt{2\phi/\pi})-\mathrm{i}S(\sqrt{2\phi/\pi})], \tag{49}$$

where the Fresnel integrals are defined as

$$S(x) = \int_0^x \sin(\pi t^2/2)\,\mathrm{d}t = \frac{1}{2} - \int_x^{\infty}\sin(\pi t^2/2)\,\mathrm{d}t,$$

$$C(x) = \int_0^x \cos(\pi t^2/2)\,\mathrm{d}t = \frac{1}{2} - \int_x^{\infty}\cos(\pi t^2/2)\,\mathrm{d}t. \tag{50}$$

It follows that for mode III

$$Q_w = -\frac{K_w}{\sqrt{2}}f(\phi), \quad f(\phi) = \sqrt{2}\left[C\left(\sqrt{\frac{2\phi}{\pi}}\right)\cos\phi + S\left(\sqrt{\frac{2\phi}{\pi}}\right)\sin\phi\right], \quad K_w = 2A\mu\sqrt{\frac{\omega}{c_2}}. \tag{51}$$

Based on (50) this function can also be represented as

$$Q_w = Q_{w0} + Q_{w1},$$

$$Q_{w0} = -\frac{K_w}{\sqrt{2}}\sin(\phi+\pi/4),$$

$$Q_{w1} = A\mu\sqrt{\frac{2\omega\phi}{\pi c_2}}\int_1^{\infty}\frac{\cos[\phi(\tau-1)]}{\sqrt{\tau}}\mathrm{d}\tau. \tag{52}$$

The expression for Q_{w0} is similar to that for modes I and II (46). It corresponds to the double, Laplace and Fourier, transform of $P^-(x,t)$, equal to $P_- = 1/S_-$ (37)

$$P^-(x,t) * * \exp[\mathrm{i}\omega(t-x/c_2)] = P_-(k,s)\exp[\mathrm{i}\omega(t-x/c_2)],$$

$$P_- = -\mu\sqrt{0+2\mathrm{i}\omega/c_2} \quad (s = 0+\mathrm{i}\omega,\ k = \omega/c_2), \tag{53}$$

and it is an asymptote of the exact expression (51) for large ϕ. The other term, Q_{w1}, rapidly tends to zero as $\phi\to\infty$

$$Q_{w1} \sim A\mu\sqrt{\omega/(2\pi c_2)}\phi^{-3/2}. \tag{54}$$

The normalized transient loading function, $f(\phi)$ (51), with its periodic asymptote, $\sin(\phi+\pi/4)$ (52), are plotted in Fig. 3.

6. Crack growth

6.1. Implicit differential equations

The relations (38), (42), (46) and (52) completely define the energy release rate based on the periodic expressions of the loading functions, while the transient solution obtained for mode III is based on the expression (51) instead of (52). Equating the energy release rate to the critical one, G_c, the following first-order ordinary differential equations are obtained:

$$G^0_{\mathrm{I,II}}(v) = \frac{\mu G_c}{(1-v)Q^2(l(t),t)} \quad \text{(modes I,II)},$$

$$G^0_{\mathrm{III}}(v) = \frac{\mu G_c}{Q^2(l(t),t)} \ \text{(mode III)}, \quad v = v(t) = \frac{\mathrm{d}l(t)}{\mathrm{d}t}, \tag{55}$$

where the expressions for $Q(l(t),t)$ depend on the fracture mode, and G^0 is defined in (38). Note that if G_c is independent of the crack speed, the right-hand side of the equation is independent of the derivative. These equations are valid, however, only for nonnegative crack speeds, and for any time-interval, when a negative crack speed is obtained, the crack tip position

must be considered as fixed, $\nu=0$. For all three modes $0 \le G^0(\nu) \le 1$, and the crack is growing when

$$Q^2 \ge \frac{\mu G_c}{(1-\nu)} \ \text{(modes I,II)}, \quad Q^2 \ge \mu G_c \ \text{(mode III)} \tag{56}$$

with the inequality (48) holding for mode I.

6.2. Crack speed-oscillation period and the time-averaged speed

In the numerical results, $\nu = \frac{1}{3}$ have been chosen unless otherwise indicated. Assuming G_c=const, it is convenient to introduce nondimensional values

$$l' = \omega l/c_R, \quad t' = \omega t, \quad \Lambda = \frac{2\mu G_c}{(1-\nu)(K_0+K_w)^2} < 1 \ \text{(modes I, II)},$$

$$l' = \omega l/c_2, \quad t' = \omega t, \quad \Lambda = \frac{2\mu G_c}{(K_0+K_w)^2} < 1 \ \text{(mode III)},$$

$$\mathcal{K}_{0(w)} = \frac{K_{0(w)}}{K_0+K_w}, \quad \mathcal{K}_0 \ge 0, \quad \mathcal{K}_w \ge 0, \quad \mathcal{K}_0+\mathcal{K}_w = 1. \tag{57}$$

In those terms, the crack growth equation is

$$G^0(V(t)) = \frac{\Lambda}{Q_0^2}, \tag{58}$$

where

$$Q_0 = \mathcal{K}_0 + \mathcal{K}_w \sin\psi, \quad \psi = t - l(t) + \pi/4, \tag{59}$$

the superscript ($'$) is omitted, and $V=v/c_R$(modes I, II), $V=v/c_2$(mode III).

The energy release functions, $G^0(V)$, for modes I and II are rather complicated. On the other hand, dependencies for the crack speed oscillations period and for the time-averaged crack speed can be obtained in general form. Each of these functions decreases monotonically from unity to zero as V increases from zero to unity. Hence an inverse function exists, $V=f(G^0)$. For modes I and II this function is plotted in Figs. 2 and 3 together with their approximations

$$V \approx f_{\mathrm{I}}(G^0) = 1 - 0.5117G^0 - 1.1459(G^0)^2 + 0.6576(G^0)^3 \quad \text{(mode I)},$$

$$V \approx f_{\mathrm{II}}(G^0) = (1 - 0.1586G^0 - 1.2967(G^0)^3)H(0.6004 - G^0) + (2.1859 - 1.5618G^0)H(G^0 - 0.6004) \quad \text{(mode II)}. \tag{60}$$

Eq. (58), which is valid for nonnegative crack speeds, can be re-arranged as

$$V(t) = Z(\psi) = f(\Lambda/Q_0^2)H(Q_0^2 - \Lambda), \tag{61}$$

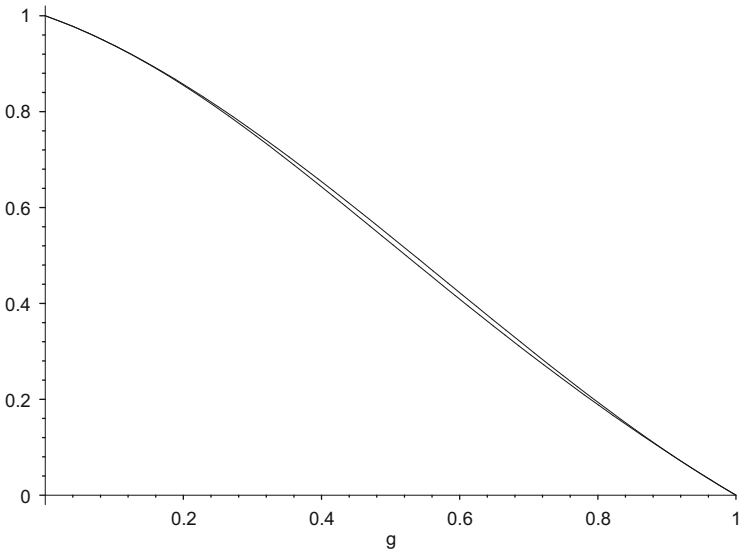

Fig. 2. Fracture mode I. The normalized crack speed, $V=v/c_R$, as a function of G^0(the lower curve) and the approximation (60) (the upper curve).

where Q_0 is defined in (59) and f is a fracture mode-dependent function. The crack speed, $V(t)$, is a periodic function. Expressions for the nondimensional period, T, and the averaged crack speed, $\langle V\rangle$, can be found from the latter equation in the following way:

$$T=\int_0^T \mathrm{d}t=\int_0^{2\pi}\frac{\mathrm{d}\psi}{1-V}=\int_0^{2\pi}\frac{\mathrm{d}\psi}{1-Z(\psi)}=\frac{2\pi}{1-\langle V\rangle},$$

$$\langle V\rangle=\frac{1}{T}\int_0^T V(t)\,\mathrm{d}t=\frac{1}{T}\int_0^{2\pi}\frac{V}{1-V}\mathrm{d}\psi=\frac{1}{T}\int_0^{2\pi}\frac{Z(\psi)\,\mathrm{d}\psi}{1-Z(\psi)}. \tag{62}$$

In accordance with (61) and (59), the support of Z can also be presented as

$$a<\psi<\pi-a \quad \text{and} \quad \pi+b<\psi<2\pi-b,$$

$$a=\Re\left(\arcsin\frac{\sqrt{\Lambda}-\mathcal{K}_0}{\mathcal{K}_w}\right), \quad b=\Re\left(\arcsin\frac{\sqrt{\Lambda}+\mathcal{K}_0}{\mathcal{K}_w}\right). \tag{63}$$

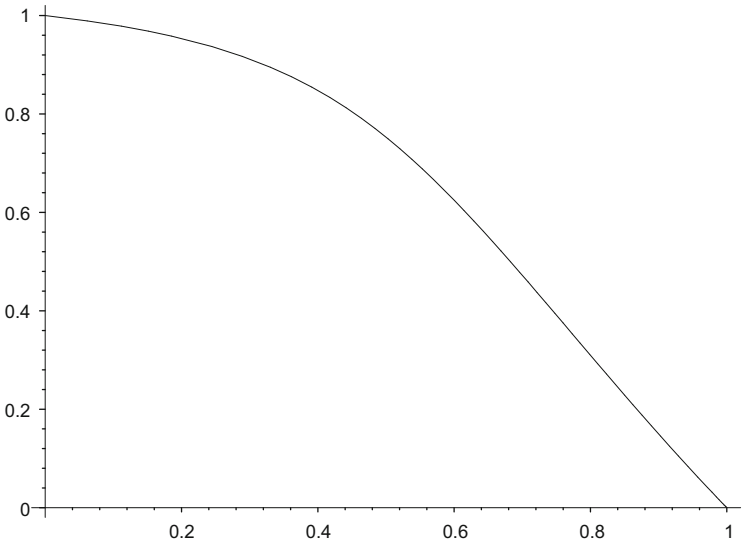

Fig. 3. Fracture mode II. The normalized crack speed, $V=v/c_R$, as a function of G^0. In the figure the 'exact' and approximate (60) curves coincide.

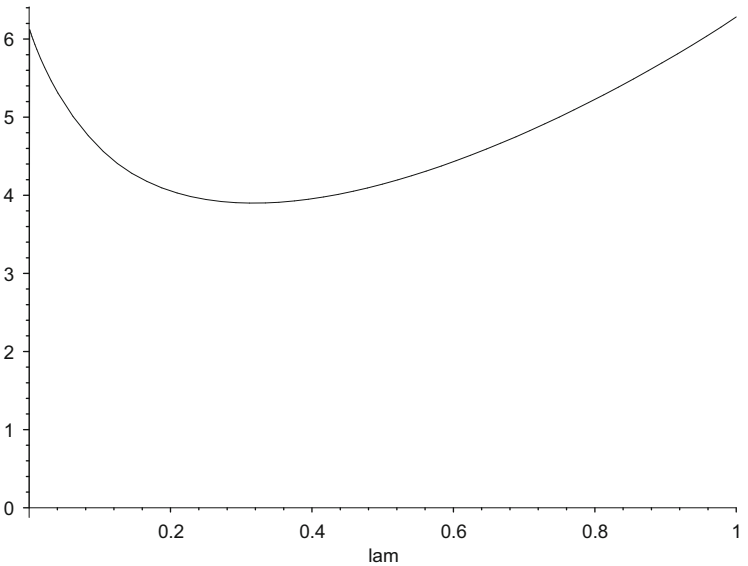

Fig. 4. Fracture mode I. The normalized time-period of the crack speed, ΛT, as a function of Λ; $K_0=\frac{2}{3}$, $K_w=\frac{1}{3}$.

Thus the averaged speed relation in (62) can also be represented as

$$\langle V\rangle = \frac{1}{T}\left[\int_a^{\pi-a}\frac{Z(\psi)\,\mathrm{d}\psi}{1-Z(\psi)}+\int_{\pi+b}^{2\pi-b}\frac{Z(\psi)\,\mathrm{d}\psi}{1-Z(\psi)}\right]. \tag{64}$$

From this, in particular, asymptotes of the period, T, and of the time-averaged speed, $\langle V\rangle$ $(\Lambda\to 0)$, can be straightforwardly found. Indeed, in this case $b\sim -a$ (63), and for modes I and II we have

$$f(0)=1,\quad f\sim 1+G^0\frac{\mathrm{d}f}{\mathrm{d}G^0}=1+\frac{1}{\mathrm{d}G^0/\mathrm{d}V}\frac{\Lambda}{Q_0^2}. \tag{65}$$

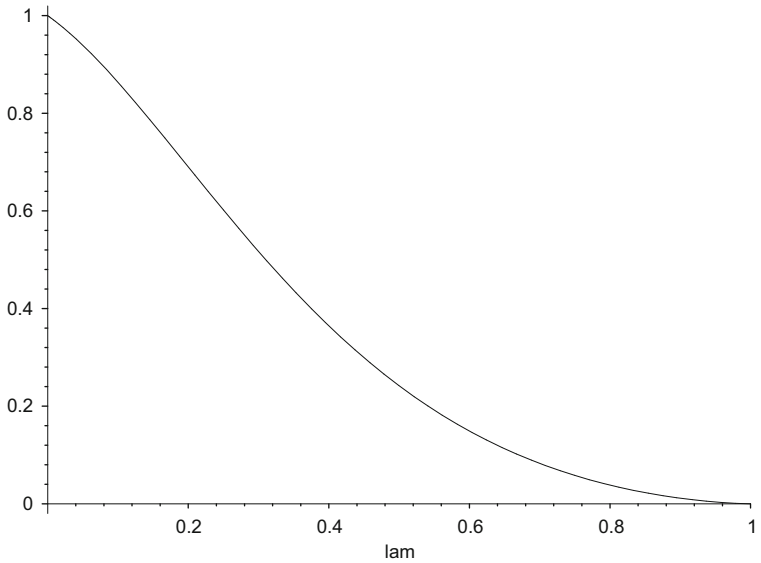

Fig. 5. The time-averaged crack speed as a function of Λ for fracture mode I; $K_0=\frac{2}{3}$, $K_w=\frac{1}{3}$.

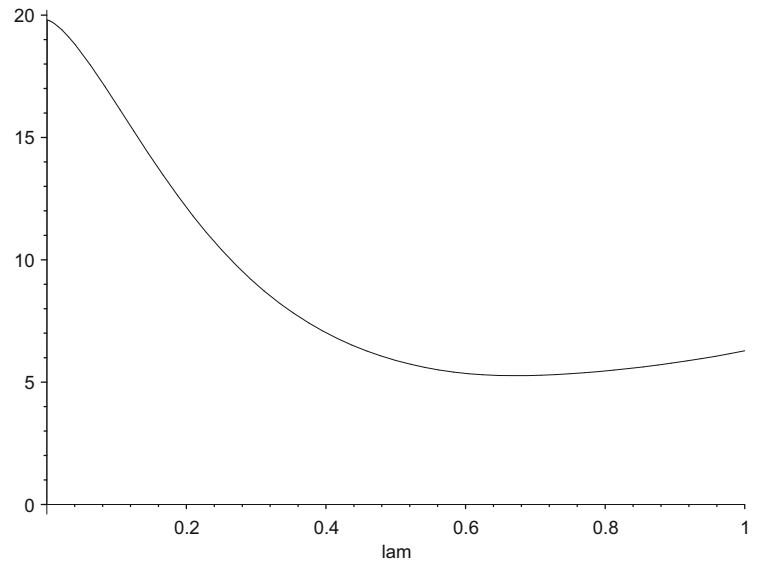

Fig. 6. Fracture mode II. The normalized time-period of the crack speed, ΛT, as a function of Λ; K_0=0, K_w=1.

It follows that

$$T\sim\int_0^{2\pi}\frac{d\psi}{1-f}=-\frac{dG^0}{dV}\frac{2\pi}{\Lambda}\left(\mathcal{K}_0^2+\frac{1}{2}K_w^2\right),$$

$$\langle V\rangle\sim\frac{1}{T}\int_0^{2\pi}\frac{f\,d\psi}{1-f}=1-\frac{\Lambda}{(-dG^0/dV)(\mathcal{K}_0^2+\frac{1}{2}K_w^2)},\tag{66}$$

where the derivatives are assumed to be taken at $G^0=0$ ($V=1$). These derivatives are found to be

$$\frac{dG^0}{dV}\approx-1.9543 \text{ mode I},\quad \frac{dG^0}{dV}\approx-6.303 \text{ mode II}.\tag{67}$$

For mode III, referring to (38), it is found that

$$f=1-\frac{2(G^0)^2}{1+(G^0)^2}=1-\frac{2\Lambda^2}{Q_0^4-\Lambda^2},\tag{68}$$

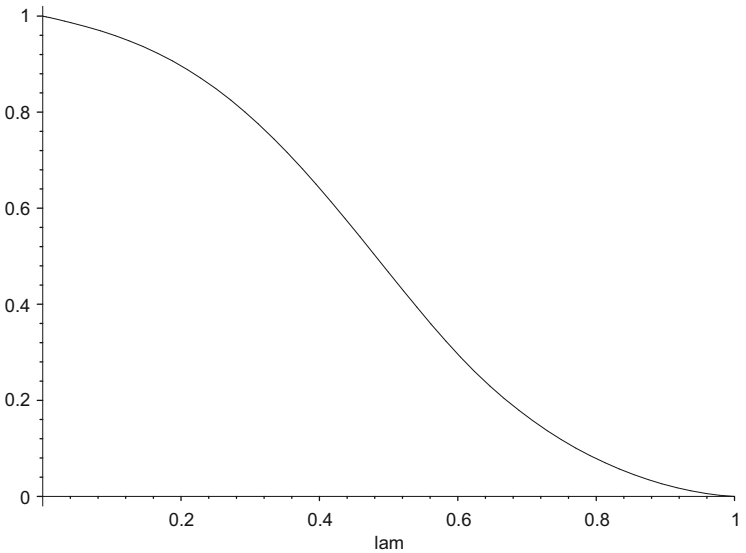

Fig. 7. The time-averaged crack speed as a function of Λ for fracture mode II, $K_0=0$, $K_w=1$.

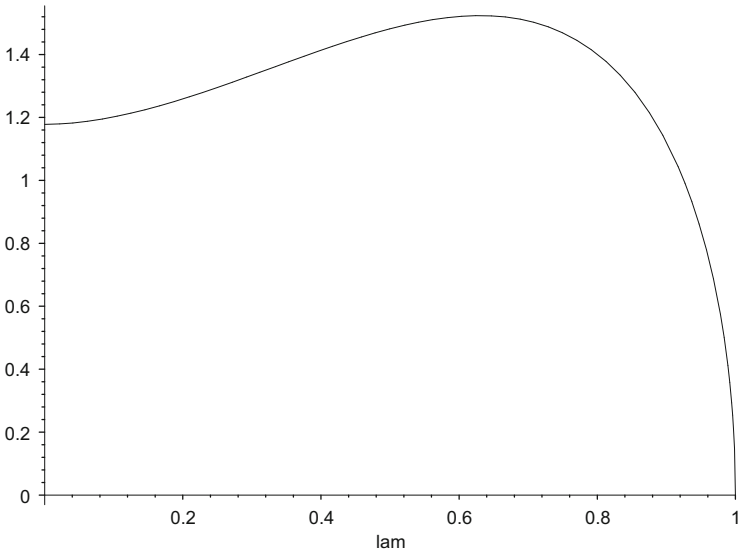

Fig. 8. Fracture mode III. The normalized time-period of the crack speed, Λ^2T, as a function of Λ; $K_0=0$, $K_w=1$.

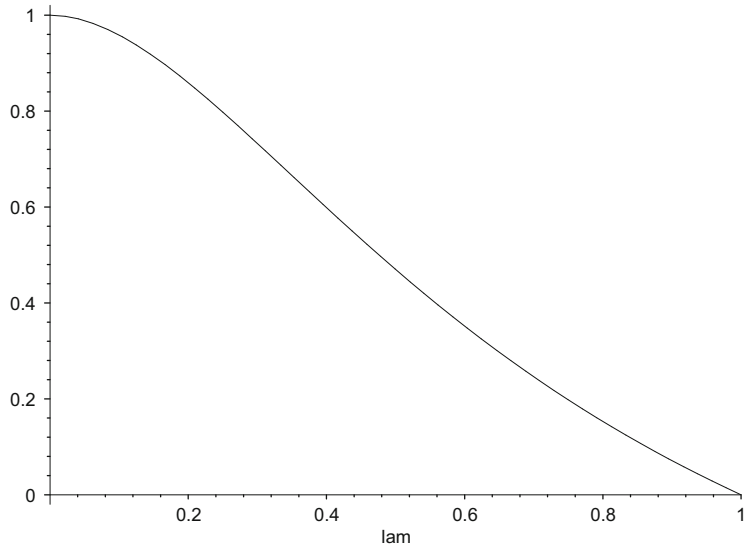

Fig. 9. The time-averaged crack speed as a function of Λ for fracture mode III, $K_0=0$, $K_w=1$.

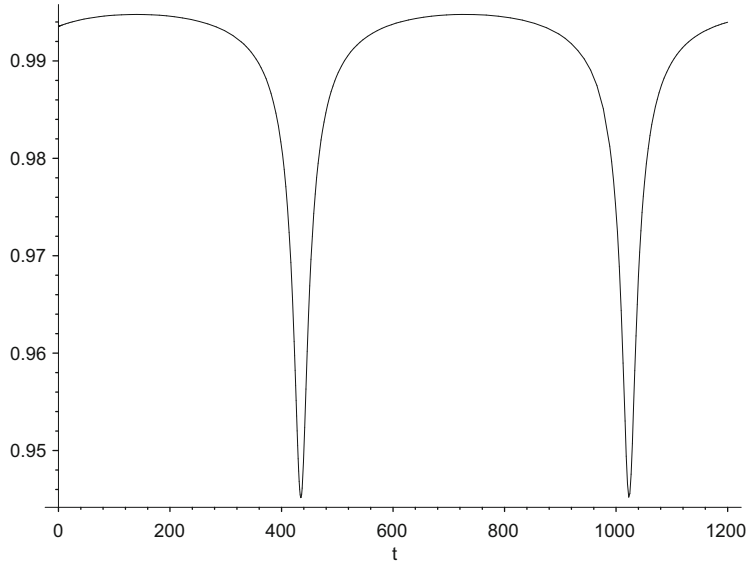

Fig. 10. Fracture mode I. The normalized crack speed, $V=v/c_R$, as a function of time; $K_0=\frac{2}{3}$, $K_w=\frac{1}{3}$, $\Lambda=0.01$.

and based on (62) the period and the time-averaged crack speed can be expressed in terms of elementary functions. The crack speed time-period and time-averaged crack speed as functions of Λ (62) are plotted in Figs. 4–9. Note that if $K_0=0$ the main period comes to half of the value defined in (62).

6.3. The explicit differential equations

Referring to (58), (59) and (38), we find the explicit differential equations based on high-accuracy approximations for modes I and II (60)

$$\frac{\mathrm{d}l(t)}{\mathrm{d}t}=f_{\mathrm{I}}\left[\frac{\Lambda}{Q_0^2}\right]H(Q_0^2-\Lambda)\quad\text{(mode I)},$$

$$\frac{\mathrm{d}l(t)}{\mathrm{d}t}=f_{\mathrm{II}}\left[\frac{\Lambda}{Q_0^2}\right]H(Q_0^2-\Lambda)\quad\text{(mode II)},$$

$$\frac{dl(t)}{dt} = \frac{Q_0^4 - \Lambda^2}{Q_0^4 + \Lambda^2} H(Q_0^2 - \Lambda) \quad \text{(mode III)}, \tag{69}$$

where the 'exact' equation corresponds to mode III. Thus, there exist two parameters here: Λ and $\mathcal{K}_0$ (for mode I the crack closure condition yields the inequality $\frac{1}{2} \le \mathcal{K}_0 \le 1$). It follows from these equations that if the wave amplitude is nonzero, $\mathcal{K}_w > 0$, then the crack speed is variable, and if

$$\mathcal{K}_0 \le \tfrac{1}{2}(1 + \sqrt{\Lambda}) \tag{70}$$

the crack grows interruptedly.

Some illustrations of the crack motion are presented in Figs. 10–15. Plots based on the transient loading function, Q_w, (51) and its periodic asymptote, Q_{w0}, (52) for mode III are presented in Fig. 16. The transient crack growth based on the transient loading function is shown in Fig. 17 (compare with Fig. 15 where the periodic regime is shown).

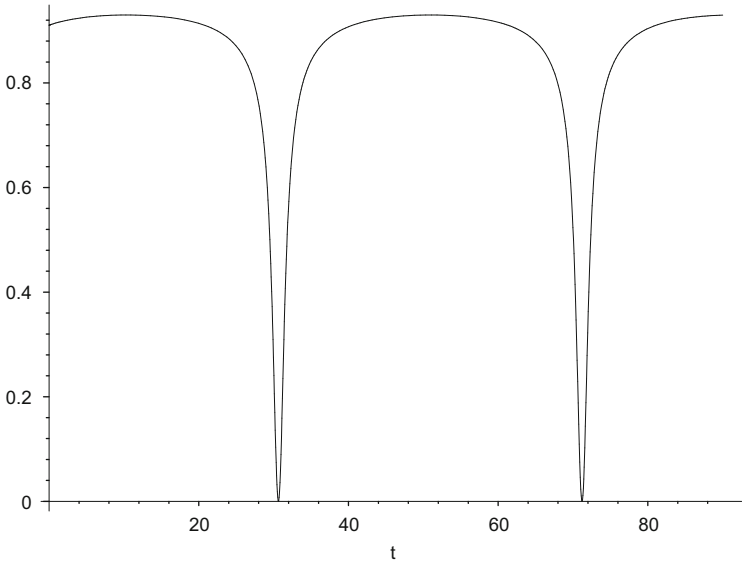

Fig. 11. Fracture mode I. The normalized crack speed, $V = v/c_R$, as a function of time; $K_0 = \frac{2}{3}$, $K_w = \frac{1}{3}$, $\Lambda = (K_0 - K_w)^2 = \frac{1}{9}$.

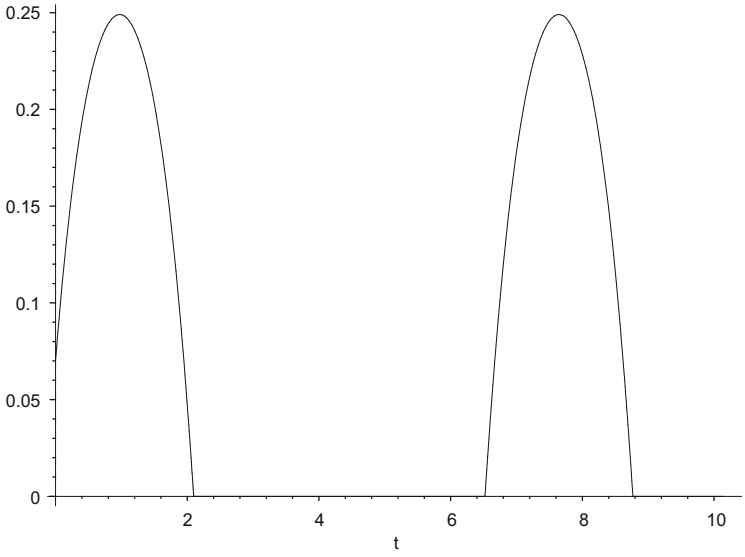

Fig. 12. Fracture mode I. The normalized crack speed, $V = v/c_R$, as a function of time; $K_0 = \frac{2}{3}$, $K_w = \frac{1}{3}$, $\Lambda = 0.75$.

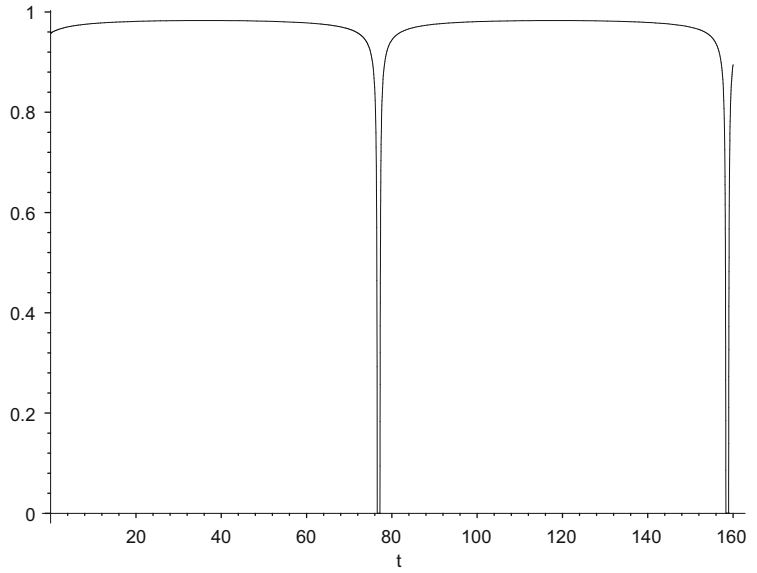

Fig. 13. Fracture mode II. The normalized crack speed, $V=v/c_R$, as a function of time; $K_0=0$, $K_w=1$, $\Lambda=0.1$.

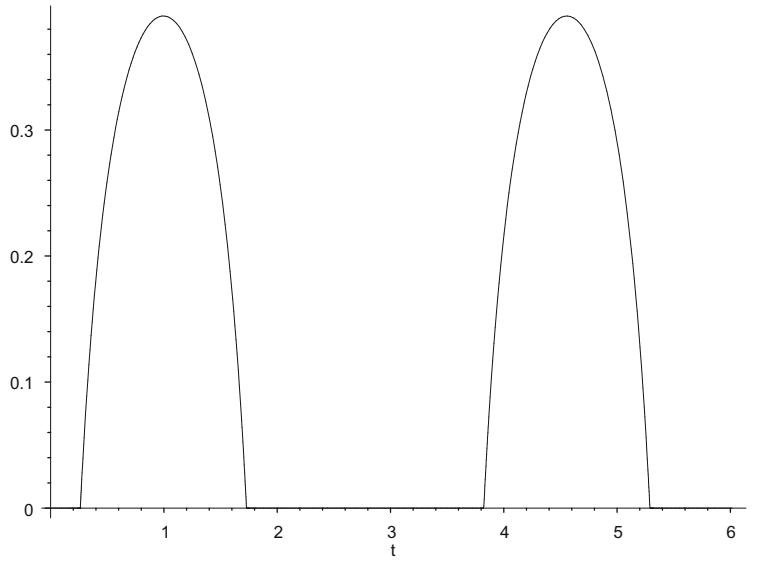

Fig. 14. Fracture mode II. The normalized crack speed, $V=v/c_R$, as a function of time; $K_0=0$, $K_w=1$, $\Lambda=0.75$.

7. Energy relations for the plane problem

The energy flux associated with a complex wave localized at the upper half-plane boundary is

$$N=\int_0^\infty \Im(\omega \boldsymbol{u}\overline{\boldsymbol{\sigma}}_x)\,\mathrm{d}y, \tag{71}$$

where σ_x is the corresponding traction vector (the stress acting from the right on the line $x=$const). Note that the complex wave is composed of two real waves of the same amplitude and frequency, and the energy flux (71) corresponds to that in these two waves. In the considered fracture problem, there also exist two real waves; one is localized at the upper half-plane boundary, and the other is localized at the lower one. Thus the total energy flux in the two real incident waves is just equal to that corresponding to the complex wave (71).

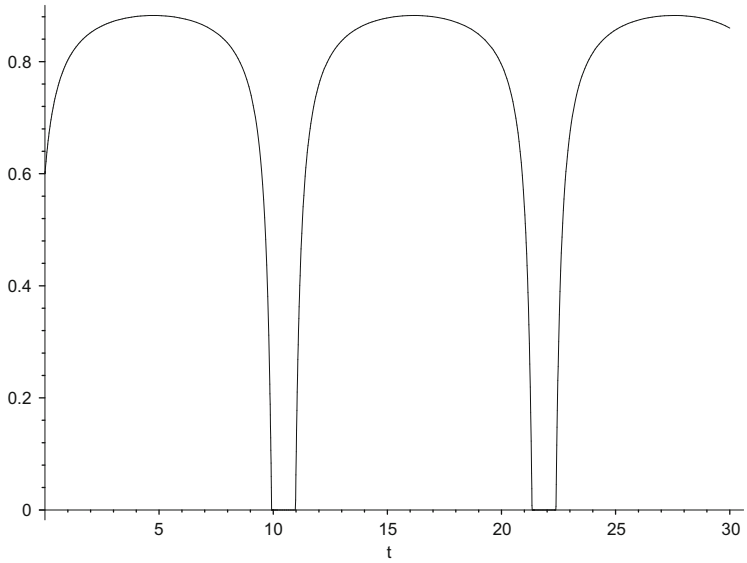

Fig. 15. Fracture mode III. The normalized crack speed, $V=v/c_R$, as a function of time; $K_0=0$, $K_w=1$, $\Lambda=0.25$.

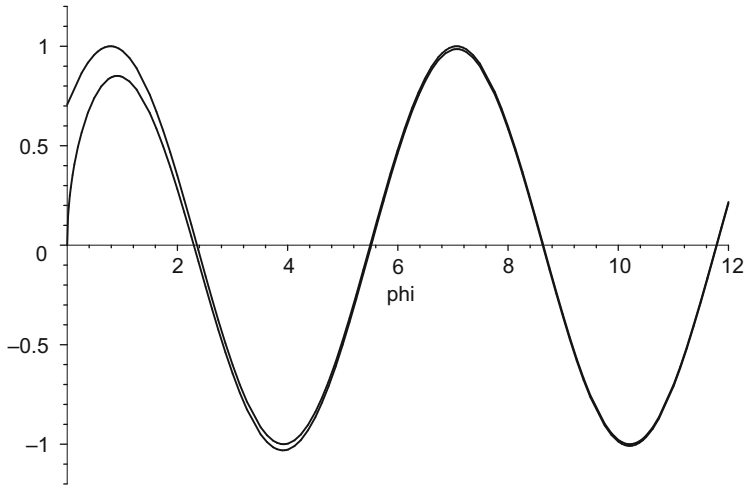

Fig. 16. Fracture mode III loading function: Transient solution, $f(\phi)$ (51), curve (1), and its periodic asymptote, $\sin(\phi+\pi/4)$, curve (2).

The complex Rayleigh wave displacements and stresses are presented in (10) and (12). Using identity (8) the energy flux can be found in a rather compact form

$$N=\mathcal{A}^2\mu\omega\frac{1-\alpha_2^2}{\alpha_1+\alpha_2}\left(1+\frac{\alpha_1-\alpha_2}{2\alpha_1\alpha_2^2}\right),$$

$$\alpha_1=\sqrt{1-c_R^2/c_1^2},\quad \alpha_2=\sqrt{1-c_R^2/c_2^2}. \tag{72}$$

In the above considerations, A is the amplitude related to the fracture mode, that is, u_y-amplitude for mode I or u_x-amplitude for mode II. In these terms, in accordance with (8), the corresponding expressions for the energy flux in the complex Rayleigh wave are

$$N=N_{\rm I}=A^2\mu\omega\frac{1-\alpha_2^2}{\alpha_1}\left(1+\frac{\alpha_1-\alpha_2}{2\alpha_1\alpha_2^2}\right)\quad\text{(mode I)},$$

$$N=N_{\rm II}=\frac{\alpha_1}{\alpha_2}N_{\rm I}\quad\text{(mode II)}. \tag{73}$$

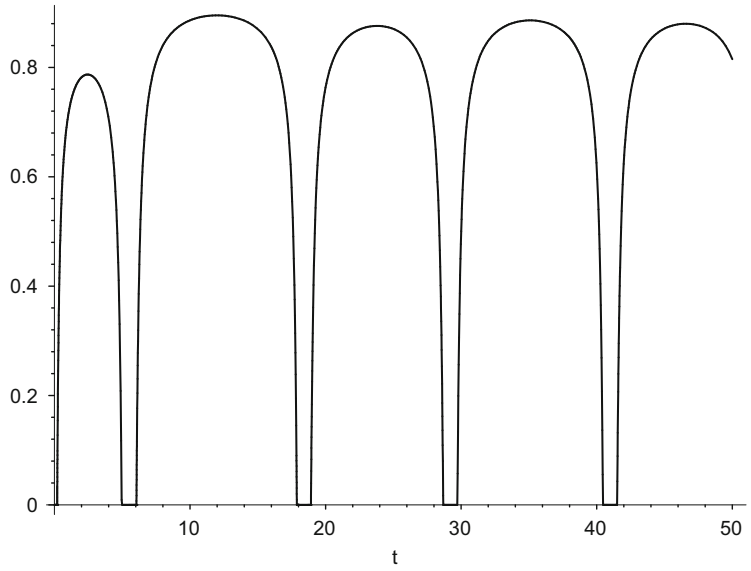

Fig. 17. Fracture mode III transient solution. The normalized crack speed as a function of time, $V=v/c_2$; $\Lambda=0.25$.

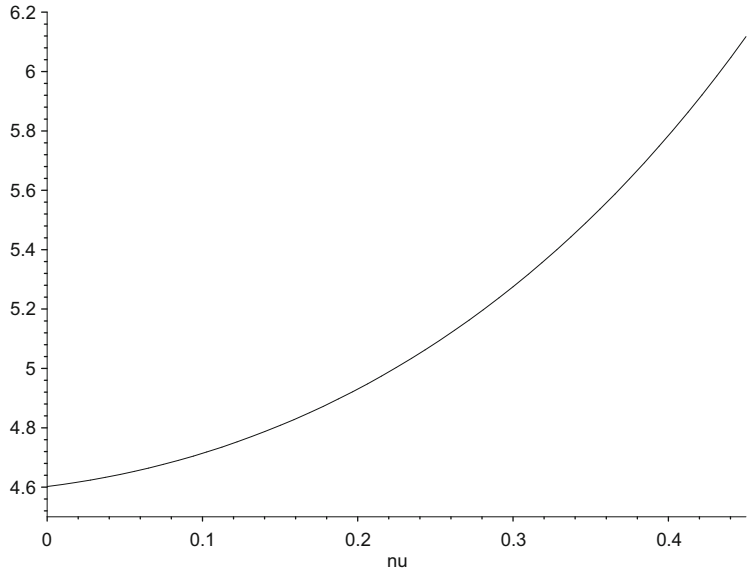

Fig. 18. The normalized energy flux in Rayleigh wave, $N/(\omega\mu\mathcal{A}^2)$, as a function of Poisson's ratio.

At the same time, the energy flux in a wave is a product of the energy density and the group velocity. In the considered case, c_R is the group velocity. Thus, the energy flux into a *free* moving-boundary domain (as if it were free), $x \geq l(t)$, $\mathrm{d}l/\mathrm{d}t=v(t)$, from the left is

$$N_v=(1-v/c_R)N \quad \text{and} \quad \langle N_v\rangle=(1-\langle v\rangle/c_R)N \ \ (v<c_R). \tag{74}$$

A part of this energy flux is spent on the fracture development; that part is given by

$$N_f=\langle v\rangle G_c \quad \text{or} \quad N_f=\langle G_c v\rangle. \tag{75}$$

The other part, N_v-N_f, goes into the reflected and scattered waves.

Referring to (46), (57), (73) and (74), the energy ratio for G_c=const is obtained as

$$\Phi=\frac{\langle v\rangle G_c}{\langle N_v\rangle}=\frac{\langle V\rangle\Lambda}{1-\langle V\rangle}\xi(v),$$

$$\xi(v)=\frac{4}{(1-v)(1+c_R/c_{1,2})D^2_{-}(c_R)}\frac{\alpha_{1,2}}{1-\alpha_2^2}\left(1+\frac{\alpha_1-\alpha_2}{2\alpha_1\alpha_2^2}\right)^{-1}. \tag{76}$$

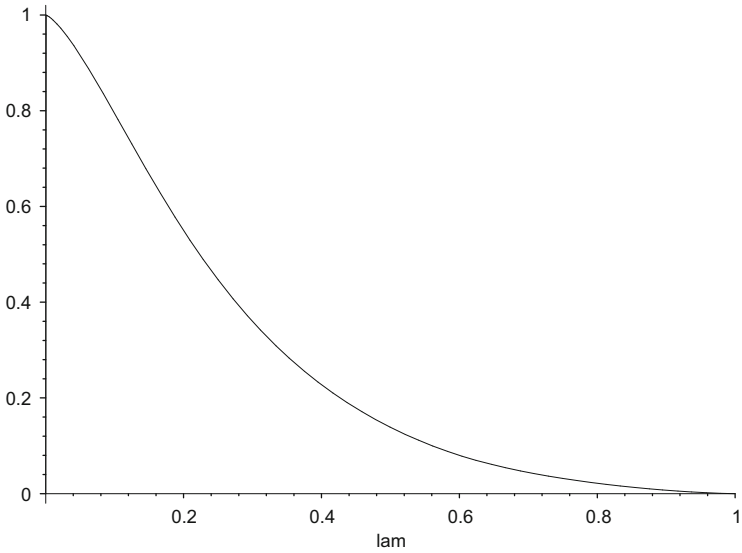

Fig. 19. The energy ratio, Φ, as a function of Λ for fracture mode II; $K_0=0$, $K_w=1$, $\nu=\frac{1}{3}$.

The normalized energy flux in the Rayleigh wave, $N/(\omega\mu\mathcal{A}^2)$, as a function of Poisson's ratio, and the energy ratio, Φ, as a function of Λ are shown in Figs. 18 and 19, respectively.

8. Some concluding remarks

As can be seen by the example of mode III (Figs. 15–17) the transient period is rather short. Note, however, that the corresponding periodic asymptotes (46), (52) are valid only for periodic regimes.

The ratio (76) shown in Fig. 19 approaches unity as the load intensity tends to infinity, $\Lambda\to 0$. This is in accordance with a one-dimensional case, where the reflective wave amplitude vanishes as the speed of an obstacle approaches the wave group velocity.

In this paper, dynamic crack growth due to the combined action of static prestress and a sinusoidal Rayleigh wave is described. At the same time, since the loading function linearly depends on the load, a Rayleigh wave of any periodic shape can also be considered. The Fourier series representation of a displacement component at $y=0$ allows both the Rayleigh wave and the loading function to be determined. In all other respects, the former way of the considerations, leading to the crack growth equation, remains valid; however, the crack speed transient period is defined by the polychromatic wave period.

In the case where the crack speed period sufficiently exceeds the transient period, space- or/and time-dependent crack resistance can also be considered based on the above-derived results. In this regard see Freund (1987, 1990).

In the same way the action of an oblique longitudinal or shear incident wave can be considered. In this case, the wave at the crack faces can have arbitrary large speed, $c>c_2$, while the crack speed is bounded.

The results of this paper can contribute, in particular, to seismology and to the theory of ultrasonic and vibroimpact cutting. The solution can also be used as the theoretical framework in the corresponding experiments. Rayleigh wave radiation by an oscillating-speed crack is among other related topics.

References

Broberg, K.B., 1999. Cracks and Fracture. Academic Press, San Diego, CA.
Fineberg, J., Gross, S.P., Marder, M., Swinney, H.L., 1991. Instability in dynamic fracture. Phys. Rev. Lett. 67 (4), 457–460.
Fineberg, J., Gross, S.P., Marder, M., Swinney, H.L., 1992. Instability in the propagation of fast cracks. Phys. Rev. B 45 (10), 5146–5154.
Fineberg, J., Marder, M., 1999. Instability in dynamic fracture. Phys. Rep. 313, 1–108.
Freund, L.B., 1972. Crack propagation in an elastic solid subjected to general loading. II. Nonuniform rate of extension. J. Mech. Phys. Solids 20, 141–152.
Freund, L.B., 1973. Crack propagation in an elastic solid subjected to general loading. III. Stress wave loading. J. Mech. Phys. Solids 21, 47–61.
Freund, L.B., 1981. Influence of the reflected Rayleigh wave on a propagating edge crack. Int. J. Fract. 17 (4), R83–R86.
Freund, L.B., 1987. The apparent fracture energy for dynamic crack growth with fine scale periodic fracture resistance. J. Appl. Mech. 54, 970–973.
Freund, L.B., 1990. Dynamic Fracture Mechanics. University Press, Cambridge, NY.
Kostrov, B.V., 1966. Unsteady propagation of longitudinal shear cracks. Appl. Math. Mech. (PMM) 30, 1241–1248.
Kostrov, B.V., 1974. Crack propagation at variable velocity. Appl. Math. Mech. (PMM) 38, 511–519.
Kostrov, B.V., 1975. On the crack propagation with variable velocity. Int. J. Fract. 11, 47–56.
Kostrov, B.V., 1976. Dynamic Propagation of Cracks with Nonuniform Speed. Mechanika Zniszczenia. Teoria i Zastosowania, Wydawn, Polskiej Acad. Nauk, Warszawa, pp. 89–122 (in Russian).
Lee, O.S., Knauss, W.G., 1989. Dynamic crack propagation along a weakly bonded plane in a polymer. Exp. Mech. 29, 342–345.

Leise, T., 2005. A general solution method for an anti-plane shear crack dynamically accelerating along a bimaterial interface. J. Mech. Phys. Solids 53, 639–653.
Marder, M., Liu, X., 1993. Instability in lattice fracture. Phys. Rev. Lett. 71 (15), 2417–2420.
Marder, M., Gross, S., 1995. Origin of crack tip instabilities. J. Mech. Phys. Solids 43, 1–48.
Mishuris, G.S., Movchan, A.B., Slepyan, L.I., 2009. Localised knife waves in a structured interface. J. Mech. Phys. Solids 57, 1958–1979, doi: 10.1016/j.jmps.2009.08.004.
Ravi-Chandar, K., 2004. Dynamic Fracture. Elsevier, Amsterdam, San Diego, Oxford.
Ravi-Chandar, K., Knauss, W.G., 1984. An experimental investigation into dynamic fracture: III. On steady-state crack propagation and crack branching. Int. J. Fract. 26, 141–154.
Rossmanith, H.P., Fourney, W.L., 1981. The reciprocal character of Rayleigh-waves and cracks. Rock Mech. 14, 37–42 (now Rock Mechanics and Rock Engineering).
Saraikin, V.A., Slepyan, L.I., 1979. Plane problem of the dynamics of a crack in an elastic solid. Mech. Solids 14, 46–62.
Slepyan, L.I., 1974. An Approximate Model of Crack Dynamics. In: Dynamics of Continua, SO Ac. Sci. USSR, No 19, pp. 101–110 (in Russian).
Slepyan, L.I., 1981. Crack propagation in high-frequency lattice vibration. Sov. Phys. Dokl. 26, 900–902.
Slepyan, L.I., 2002. Models and Phenomena in Fracture Mechanics. Springer, Berlin.
Slepyan, L.I., Fishkov, A.L., 1980. Mixed plane problems for nonuniform movement of boundary conditions alternation point. In: Contemporary Problems in Mechanics of a Continuum, LGU, No. 13, pp. 172–181 (in Russian).
Slepyan, L.I., Mishuris, G.S., Movchan, A.B., 2009. Crack in a lattice waveguide. Int. J. Fract., doi:10.1007/s10704-009-9389-5.
Walton, J.R., Herrmann, J.M., 1992. A new method for solving dynamically accelerating crack problems: part 1. The case of a semi-infinite mode III crack in elastic material revisited. Q. Appl. Math. L (2), 373–387.
Willis, J.R., 1990. Accelerating cracks and related problems. In: Eason, G., Ogden, R.W. (Eds.), Elasticity, Mathematical Methods and Applications. Ellis Horwood Ltd., Chichester, pp. 397–409.
Willis, J.R., Movchan, A.B., 1997. Three-dimensional dynamic perturbation of a propagating crack. J. Mech. Phys. Solids 45, 591–610.